A 3D ear recognition method based on auricle structural feature

Kai Wang, Zhi-chun Mu

School of Automation and Electrical Engineering, University of Science and Technology Beijing, Beijing, 100083, China

Abstract

The performances of most existing 3D ear recognition methods are degraded sharply by pose variation. In this paper, a 3D ear representation called 3D auricle structural feature(3DASF) and the corresponding pose robust 3D ear recognition method is presented. By measuring the surface characteristics through Surface Variation, 3DASF that contains ear key physiological structure is extracted. Then 3DASF corresponding points are used to implement iterative closest point(ICP) algorithm to coarse align gallery-probe ear pairs. Finally, fine alignment is performed to obtain the alignment errors for identity recognition. Experimental results conducted on University of Notre Dame(UND) biometric datasets collection F and collection G outperform the state-of-the-art 3D ear recognitions based on ICP. The results also demonstrate that the proposed method is more robust to pose variation than the state-of-the-art.

Keywords: *3D ear recognition, 3D feature extraction, auricle structure, iterative closest point.*

1. Introduction

Biometric system uses human physiological characteristics, such as face[1], fingerprint, iris etc., as well as behavioral characteristics, such as gait, handwriting, voice authentication etc., which can not easily be stolen and counterfeited. As a biometric trait, the human ear, has the common characteristics of biometric traits, such as universality, uniqueness, permanence etc. , has a rich and stable structure, and unlike the face which is variable under different scenario such as expression variation, aging, makeup and eyeglasses, is receiving more and more attentions. Ear recognition based on 2D images in constrained condition has attained the accuracy of 90% , however, 2D images of the human ear is susceptible to variation in illumination and pose, greatly affecting the recognition accuracy. The research of Chang and Bowyer show that ear recognition based on 2D images is greatly affected by pose variation, even reduced to below a accuracy of 30%[2]. How to improve the accuracy in the case of pose variation is one of hot issues in theory and application of ear recognition.

Using the commercial 3D laser scanner to obtain the 3D shape of human ear for recognition, which exploits the depth information, also is propitious to overcome the problems such as illumination and pose variation. In the literatures about 3D ear recognition, ICP[3] is most widely used, that is a classical method of 3D point cloud registration. Thus, the most of early research work are testing and evaluating the different variants of ICP applied to 3D ear recognition[4-9]. Recently, the framework of 3D ear recognition utilizing 3D feature extraction has gained much attentions. Bir Bhanu et al. put forward the LSP (Local Surface Patch) descriptors[10], which has shown good results in free form object classification, and successfully applied to 3D ear recognition[11-13]. Islam et al. employ local 3D features to achieve coarse alignment of 3D ears. Moreover, a large number of non candidate samples can be excluded according to the alignment errors[14]. The aforementioned researchers both use the extracted local surface features to obtain the ear corresponding points, but a satisfactory recognition accuracy is difficult to be obtained when only the corresponding points between ear samples are used according to the experiment results. In order to make good use of the acquired corresponding points, the coarse alignment of point cloud is performed with these points, then fine alignment is done with ICP algorithm, thus good recognition accuracy can be achieved. Zhou et al.[15] propose the Surface Patch Histogram of Indexed Shapes (SPHIS) 3D feature descriptors for local ear surface representation and matching, then voxelization is used to holistic matching, finally the scores from local and holistic match components are fused to generate the final scores. Comparing to the Hui[11] and Islam[14], Zhou et al.' method achieves better results.

The methods of 3D ear recognition based on 3D feature extraction improve the computational efficiency, however, good performances only can be achieved in datasets with pose nearly invariability. In the occasion of pose variation, those methods perform not well. Aiming to this problem, we propose a new 3D ear feature for recognition-- 3D auricle structural feature(3DASF) and the corresponding

3D ear recognition method. The coarse alignment is efficiently carried out with the 3DASF points, then ICP fine alignment is performed to obtain the alignment error. The experiments on University of Notre Dame(UND) biometric datasets collection F and collection G are performed to evaluate the proposed method. Comparisons with state-of-the-art methods are performed to illustrate the applicability of the proposed method.

The rest of paper is organized as follows. The 3D auricle structural feature is described in Section 2. The 3D ear recognition based on auricle structural feature is explained in Section 3. The performance of the proposed method is evaluated and compared with other approaches in Section 4. Finally, Section 5 gives the conclusions.

2. 3D Auricle Structural Feature

The performance of a biometric recognition system directly depends on how to represent the data and how to extract the important feature from the representation of data. Ear has abundant ridges and channels which are shown as the concave and convex surface. Meanwhile, the key physical structure of ear, such as helix, antihelix, earlobe, etc. mostly are located at the vertices of the convex or concave surface, which can be seen from Figure 1. The different colors represent the variation of ear surface depth. If the depth variation can be estimated, based on this, the surface vertices can be classified into different types, and the key physical structure could be extracted.

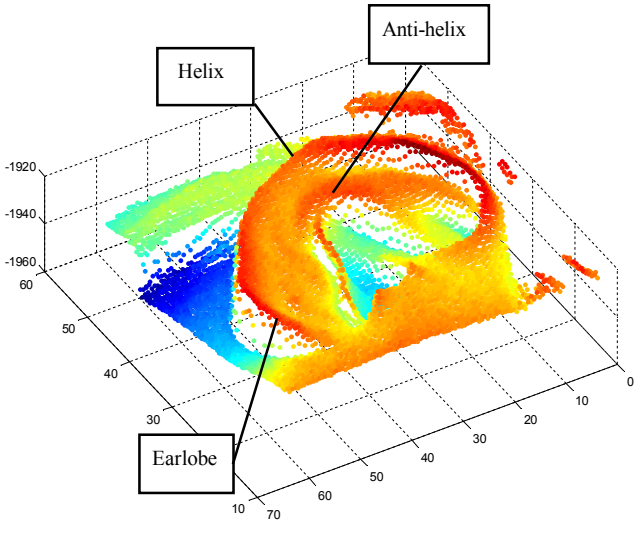

Fig. 1 3D auricle structure

2.1 Representation of 3D ear and local neighborhood of vertex

Generally, 3D data is represented and storaged by point cloud or mesh. The point cloud produced by 3D laser scanner can be used to construct mesh to obtain more compact storage and representation. The experimental data used in this paper comes from the University of Notre Dame, UND biometrics dataset, collection F and collection G[16], which was collected using Minolta Vivid 910 laser scanner. All the data in UND dataset are single scanning point clouds. The single scanning point cloud of ear from a singe view usually has self occlusion, nevertheless, the parts that are prone to be self occluded often are located at cavum conchae and the concave surface between helix and antihelix, that will not have a crucial impact to the completeness of the key physical structure of ear. Therefore, we first uniformly resample the raw point cloud, and use grid fitcode from mathworks website[17] to conduct surface fitting to transform point cloud into depth lattice array. Then mesh representation of 3D ear which has not geometrical sudden changes and still be consistent with the 3D ear shape ground truth is obtained by triangulation, as shown in Figure 2.

In order to estimate the variation of depth, the neighborhood of 3D mesh vertices is defined as follow. For a mesh vertices v_0, a set of rings can be defined around it, the first ring R_1 includes all immediate neighbors of the vertices v_0, the second ring R_2 including the all immediate neighbors of the vertices in the first ring c and so on. The c-th ring R_i can be defined in the following condition: for one vertex v of i-th ring c, there exists a shortest path from v_0 to c that contain i

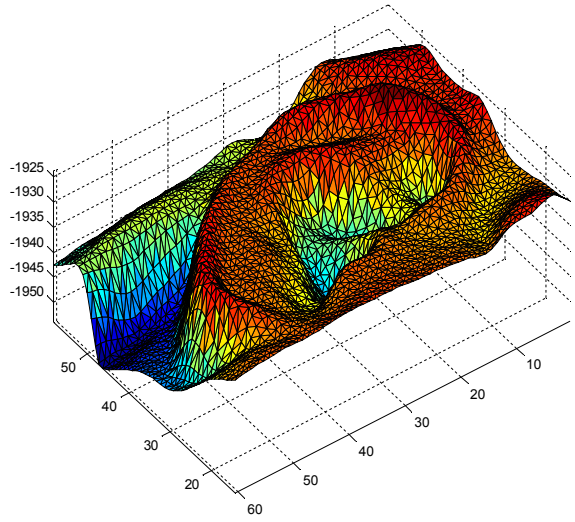

Fig. 2 The mesh representation of a 3D ear

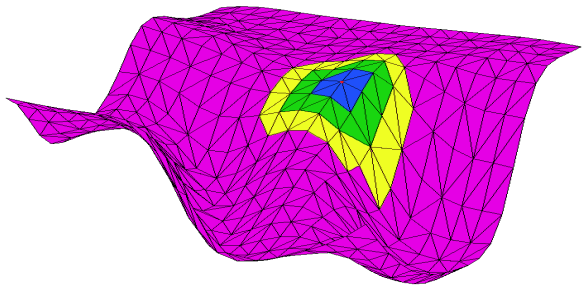

Fig. 3 3-ring neighborhood. The meshes in 3 rings are shown with different colors.

edges, then the set $\Re = \{R_i : i \le N\}$ is defined as the N-ring on the vertices v_0. Figure 3 shows a 3-ring neighborhood around a mesh vertex.

2.2 Surface Variation

Eigenvalues of the covariance matrix of a local surface neighborhood can be used to estimate the surface properties[18, 19]. A vertex of 3D mesh and its N-ring neighborhood vertices is given by $p_i = [x_i \ y_i \ z_i]^T$ $(i = 1, \ldots, n_l)$, then the covariance matrix is given by:

$$C = \begin{bmatrix} p_{i_1} - \overline{p} \\ \cdots \\ p_{i_k} - \overline{p} \end{bmatrix}^T \cdot \begin{bmatrix} p_{i_1} - \overline{p} \\ \cdots \\ p_{i_k} - \overline{p} \end{bmatrix}, \quad i_j \in N_p \qquad (1)$$

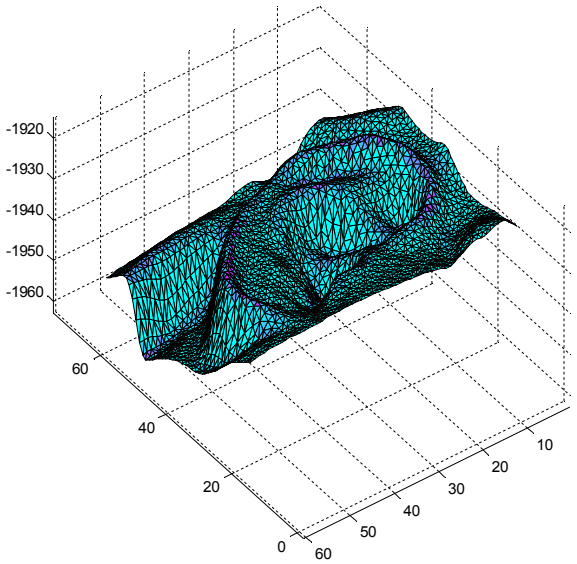

Fig. 4 3D auricle structural feature base on surface variation, as shown in purple.

Where $\overline{p}$ is centroid of the neighbors p_{i_j}, eigenvectors v_l can be obtained through eigenvalue decomposition of covariance matrix C by Principal Component Analysis(PCA). $C \cdot v_l = \lambda_l \cdot v_l, l \in \{0,1,2\}$.

C is a symmetric and positive semi-definite matrix, all the eigenvalues λ_l are real numbers, eigenvectors v_l consist an orthogonal basis corresponding to the primary components of vertices set N_p. v_l measure the variation of p_i, $i \in N_p$ along the direction of corresponding eigenvectors. The total variation is defined as sum of the square distance between p_i and its centroid:

$$\sum_{i \in N_p} \left| p_i - \overline{p} \right|^2 = \lambda_0 + \lambda_1 + \lambda_3 \qquad (2)$$

Pauly et al.[20] defines the Surface Variation(SV) $\sigma_n(p)$ on the local surface that can quantitatively measure the variation.

$$\sigma_n(p) = \frac{\lambda_0}{\lambda_0 + \lambda_1 + \lambda_2} \qquad (3)$$

Where $\lambda_0 \le \lambda_1 \le \lambda_2$. If $\sigma_n(p) = 0$, then all the vertices are located on a plane. When the neighborhood are the vertices with the isotropically distribution, $\sigma_n(p)$ can attain the maximum 1/3.

Based on (3), SV of every vertices of the 3D ear surface can be computed and are shown in Figure 4 with different colors. It is observed that SV of the key structures of 3D ear such as helix, antihelix, tragus, concha etc. have high values, therefore, selecting the appropriate σ_t, the expected feature vertices p could be detected based on the principle $\sigma_n(p) > \sigma_t$ .In the following, 3-ring neighborhood is used, where $\sigma_t = 0.02$ in experiment 1 and experiment 2, 2-ring neighborhood is used, where $\sigma_t = 0.04$ in experiment 3.

3. 3D ear recognition based on auricle structural feature

The proposed 3DASF include the key physical ear parts and greatly reduces the dimensionality compared to the original data. In this section, the 3D ear recognition based on 3DASF is described, 3DASF is first used to coarsely align the probe gallery ear pairs, then fine alignment is performed with ICP.

3.1 Coarsely align the probe gallery ear pairs based on 3DASF

Let 3DASF point set of the probe ear be M, 3DASF point set of the gallery ear be U, the ICP algorithm is performed between the feature point sets in order to obtain the spatially closest points, which lead to rigid transformation α making error between two points sets minimum. The initial transformation α^0 is set to be the translational transformation of the centroids of two point sets.

The centroids of two point sets are given by

$$C_M = \frac{1}{n}\sum_{i=1}^{n} m_i , \quad C_U = \frac{1}{n}\sum_{i=1}^{n} u_i \tag{4}$$

then,

$$\alpha^0 = C_M - C_U \tag{5}$$

The algorithm starts with the initial transformation α^0, and iteratively calculates α^k until converges. In each iteration, the correspondences between two point sets are obtained by looking for the closest points, then the mean square error(MSE) $E(\alpha^*)$ between two point sets is minimized to reach a certain threshold.

The k-th iteration process of ICP algorithm:

(1) Find the closest point set $U^k = \{u_1^k, u_2^k, \ldots, u_n^k\}$ of the point set M^k;

(2) Using SVD to calculate rigid transformation α^k, make $\alpha^k(M^k)$ closest to U^k, i.e. minimizing $E(\alpha^k) = \frac{1}{n}\sum_{i=1}^{n}\left\|\alpha^k(m_i^k) - u_i^k\right\|^2$;

(3) Applying rigid transformation α^k to point set M^k to get point set M^{k+1}, i.e. $M^{k+1} = \alpha^k(M^k)$;

(4) If the difference of MSE $E(\alpha^*)$ between two iterations is below a threshold or exceed a limit number of iteration, i.e. $E(\alpha^{k-1}) - E(\alpha^k) < \tau$, the iteration stop; Otherwise, goto step1 and $k+1$-th iteration continue.

By performing ICP algorithm above, rigid transformation α and MSE $E(\alpha)$ between two closest point sets can be obtained, where α can regarded as the initial transformation of the subsequent ICP algorithm of fine alignment. The attempt to do ear recognition using only $E(\alpha)$ is also tested, which is described in section 4.

3.2 The ICP fine alignment of 3D ear

The obtained rigid transformation is used as the initial transformation which is applied to the probe gallery ear pairs, then the ICP algorithm is used to match the probe ear and gallery ear. The gallery ear which has the minimum error with the probe ear will be considered to be the recognition result.

An important step of ICP algorithm is to find the spatially closest point, however, a point in point set X may have one or multi closest point in points set Y. Even if the distance is the shortest, the point may not be the real closest point. Thus, during the process of calculating the rigid transformation, only the point whose distance to its correspondence is less than a threshold τ is selected to calculate the rigid transformation. Generally, τ is set to be the average distance between two point sets plus the double R, R is the resolution of the surface of probe ear.

For the reason that the oiliness of human skin, sensor error and so on, the 3D data from 3D scanner inevitably contains noise, which will lead to "many to one" in the process of finding the closest point. Therefore, the distances between corresponding points are calculated and sorted to select the minor 75% of the distance to update the average distance of two point sets, after several iterations, the effect of noise points will gradually be eliminated.

Finally, the alignment errors are ranked to choose the gallery ear with the smallest error as the recognition result.

4. Experiment

The experimental data comes from UND biometrics datasets collection F and collection G, total of 1,800 3D point cloud data (with the corresponding color images). The data is from 415 individuals, each with 2 or more than 2 (2D color images and the corresponding 3D data), including 237 males, 178 females, there are 70 people with earrings, 40 people ear slightly obscured by hair. A subset of collection G is comprised of 24 people whose images are taken at four different poses, 15° off center, 30° off center, and 45° off center and used to evaluate the impact of pose variation on the performance of recognition algorithm. Figure 5 shows some cases of 3D depth map.

In UND biometrics datasets, collection F and collection G, 2D color image and 3D depth map is registered, so we use Adaboost method [21] to automatically detect and locate ear area in 2D color images, and crop the corresponding area in 3D depth map. In a few cases of automatically ear detection not working, we manually crop ear area. The

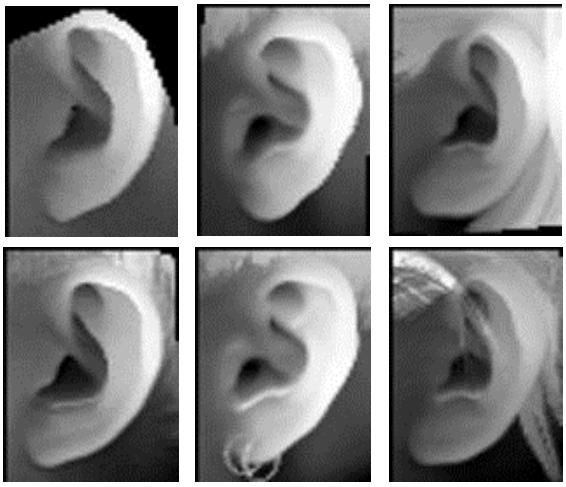

(a)Pose (b) Earing (c) Occlusion

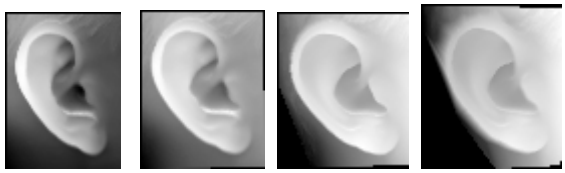

(d)Pose variation

Fig. 5 Ear range images

cropped 3D ears are divided into two sets: galley set 1 and probe set 1, each set has 415 point clouds randomly selected from 415 individuals. In the pose variation subset of 24 subjects, the subjects with same pose make up a micro subset. Every image of each micro subset will be matched against all the images from other micro subsets.

Except the adaboost method, all other algorithms are implemented on Intel Xeon (R) CPU 2.4GHz, 12.0G RAM, Maltab 7.12.0 (R2011a).

In order to validate the proposed 3DASF for ear, we first try to only use 3DASF to carry out 3D ear recognition on galley set 1 and probe set 1. The ICP algorithm described in section 3.1 is used to align the 3DASF points of probe ear and gallery ear. The candidate ear which has the minimum MSE with probe ear will be considered as the recognition result. Cumulative Match Characteristics (CMC) is used to evaluate the performance. The results is shown in Table 1. The limit number of ICP algorithm iteration is set to be 30 times, iterative threshold $\tau = 1 \times e^{-4} mm$.

Table 1: CMC of only using 3DASF

Rank-1	Rank-2	Rank-3	Rank-4	Rank-5
77.59%	79.52%	82.17%	82.41%	82.89%

The rank-1 recognition rate is only 77.59% when 3DASF is used alone. The reason can be summed up that the 3DASF usually contain noise points of the background area, when background of probe ear and gallery ear change greatly, the error will be sharply increased that degrade the recognition rate.

Table 2 shows the CMC of coarsely aligning the probe gallery ear pairs, and then ICP fine alignment is performed on galley set 1 and probe set 1. Since the extracted 3DASF of ear contains important physiological region, a good initial rigid transformation can be obtained after coarsely aligning the probe gallery ear pairs. Then, ICP algorithm is used for fine alignment, that can get a better recognition performance compared with directly using ICP fine alignment. The Rank-1 recognition rate is 97.59%. The limit number of ICP algorithm iteration is set to 30 times, iterative threshold $\tau = 1 \times e^{-4} mm$.

Table 2: CMC of "coarsely aligning the probe gallery ear pairs with 3DASF + ICP fine alignment"

Rank-1	Rank-2	Rank-3	Rank-4	Rank-5
97.59%	98.55%	99.04%	99.04%	99.04%

In order to solve the pose problem which can not be overcame with 2D recognition approach, the proposed 3D ear recognition method based on 3DASF is evaluated on the pose variation subset for robustness on the occasion of pose variation. The four micro subsets are considered as the gallery set and the probe set in turns, and cross matched against each other. The results are shown in Table 3. It can be observed that the results obtained by the proposed method are better than Hui[11]'s, Yan[22]'s and Zhou[15]'s at the mean value of rank-1 rate. The relative invariability of the 3DASF is shown and the proposed method is with robustness to pose variation to some extent.

The comparison of our method and other 3D ear recognition method is shown in Table 4. The proposed method needs less matching time and achieves higher preferred recognition rate than other method which are based on ICP algorithm. Compared with Zhou's method, although its match time and the recognition rate are better, but the extraction process of SPHIS local feature is relatively complex, involving feature point selection, surface curvature calculation and so on, thus its computation time can not be ignored. Zhou did not mentioned the time cost of SPHIS local feature extraction. With the same principle with Zhou' work, Islam' L3DF can be used as a reference to SPHIS. L3DF ear feature extraction time for a single person is 22.2 seconds. By comparison with that, the proposed 3DASF extraction time is 1.11 seconds, which has an obvious advantage.

Table 3 Comparison among this paper's method and others on the subset with pose variation of Collection G

Gallery / Probe	90°	75°	60°	45°	Average
90°		**100**% [100%, 100%, 100%]	**95.8**% [87.5%, 87.5%, 87.5%]	**87.5**% [83.3%, 70.8%, 70.8%]	**94.4**% [90.3%, 86.1%, 86.1%]
75°	**100**% [100%, 100%, 100%]		**100**% [100%, 100%, 100%]	**91.7**% [91.7%, 87.5%, 83.3%]	**97.2**% [97.2%, 95.8%, 94.4%]
60°	**100**% [91.7%, 87.5%, 91.7%]	**100**% [100%, 100%, 100%]		91.7% [91.7%, **95.8**%, 87.5%]	**97.2**% [94.4%, 94.4%, 93.1%]
45°	83.3% [**87.5**%, 79.2%, 58.3%]	**91.7**% [87.5%, 87.5%, 83.3%]	95.8% [87.5%, **100**%, 83.3%]		**90.3**% [87.5%, 88.9%, 75%]
Average	**94.4**% [93.1%, 88.9%, 83.3%]	**97**% [95.8%, 95.8%, 94.4%]	**97.2**% [91.7%, 95.8%, 90.3%]	**90.3**% [88.9%, 84.7%, 80.5%]	**94.8**% [92.4%, 91.3%, 87.1%]

Hui[11]'s, Yan[22]'s and Zhou[15]'s results are given in the brackets. The better recognition results are bolded.

Table 4: Comparison with other 3D ear recognition methods

Authors	Preprocess	Methods	Time of feature extraction(one person)	Matching time	Rank-1
Yan[22]	Skin detection + Ear hole location + Active Contour Model	ICP(415 person)	N/A	5~8 s	97.6%
Chen[11]	Skin detection + Edge extraction + Reference Ear Shape Model	LSP + ICP(302 person)	3.7 s		96.36%
Zhou[15]	HIS ear location	SPHIS+ Voxelization(415 person)	Not reported	0.02 s	98.3%
Islam[14]	Adaboost ear detection	L3DF+ICP(415 person)	22.2 s	2.28 s	93.5%
This paper	Adaboost ear detection	3DASF+ICP(415 person)	1.11 s	0.22 s	97.59%

5. Conclusion

This paper propose a new 3D ear representation for recognition--3DASF and the corresponding 3D ear recognition method. The 3DASF extraction is based on the estimating the variation of mesh surface, which contains the important information about ridge and channel of ear. 3DASF is used for coarsely alignment and further ICP algorithm is used for fine alignment. The better recognition performance than the existing recognition method based on ICP algorithm is achieved. The experiment on UND biometrics datasets collection F and collection G from 415 individuals shows that the rank-1 recognition rate is 97.59%, and feature extraction and matching time is respectively 1.11 seconds and 0.22 seconds. The experiment on the pose variation subset of collection G shows the robustness of the proposed method to pose variation.

The low recognition rate when only using 3DASF is discovered in the experiment. Therefore, in the future work, how to overcome the effect of background noise, extract more accurate and efficient 3D structure feature to

form a better recognition solution with flexibility is a open problem.

Acknowledgments

The authors are grateful to computer vision research laboratory at University of Notre Dame for providing UND biometrics datasets, collection F and collection G.
This work is supported the Natural Science Foundation of China under grant no. 60973064, the Doctoral Fund of Ministry of Education of China under grant no. 20100006110014, and the Beijing Municipal Natural Science Foundation under grant no. 4102039

References

[1] M. K. J. R.Rajalakshmi, "A review on classifiers used in face recognition methods under pose and illumination variation", International Journal of Computer Science Issues, vol.9, no.6 2012, pp. 474~485.
[2] C. Kyong, K. W. Bowyer, S. Sarkar and B. Victor, "Comparison and combination of ear and face images in appearance-based biometrics", Pattern Analysis and Machine Intelligence, IEEE Transactions on, vol.25, no.9 2003, pp. 1160-1165.
[3] P. J. Besl and N. D. McKay, "A method for registration of 3-d shapes", Pattern Analysis and Machine Intelligence, IEEE Transactions on, vol.14, no.2 1992, pp. 239-256.
[4] Y. Ping and K. W. Bowyer, "Ear biometrics using 2d and 3d images", in Computer Vision and Pattern Recognition - Workshops, 2005. CVPR Workshops. IEEE Computer Society Conference on, 2005, pp. 121-121.
[5] P. Yan and K. W. Bowyer, "A fast algorithm for icp-based 3d shape biometrics", Proc. Proceedings of the Fourth IEEE Workshop on Automatic Identification Advanced Technologies2005, pp. 213-218.
[6] P. Yan and K. W. Bowyer, "Empirical evaluation of advanced ear biometrics", in Computer Vision and Pattern Recognition - Workshops, 2005. CVPR Workshops. IEEE Computer Society Conference on, 2005, pp. 41-41.
[7] P. Yan, K. W. Bowyer and K. J. Chang, "Icp-based approaches for 3d ear recognition", 2005, pp. 282-291.
[8] H. Chen, B. Bhanu and R. Wang, "Performance evaluation and prediction for 3d ear recognition", in Audio- and video-based biometric person authentication, eds. T. Kanade, A. Jain and N. Ratha, pp. 748-757, Springer Berlin Heidelberg, 2005.
[9] P. Yan and K. W. Bowyer, "An automatic 3d ear recognition system", in Proc. Third Int'l Symp. 3D Data Processing, Visualization, and Transmission, 2006, pp. 213-218.
[10] H. Chen and B. Bhanu, "3d free-form object recognition in range images using local surface patches", Pattern Recogn Lett, vol.28, no.10 2007, pp. 1252-1262.
[11] C. Hui and B. Bhanu, "Human ear recognition in 3d", Pattern Analysis and Machine Intelligence, IEEE Transactions on, vol.29, no.4 2007, pp. 718-737.
[12] C. Hui and B. Bhanu, "Efficient recognition of highly similar 3d objects in range images", Pattern Analysis and Machine Intelligence, IEEE Transactions on, vol.31, no.1 2009, pp. 172-179.
[13] K. Wang, Z. Mu and Z. He, "An efficient approach of 3d ear recognition", in 10th World Congress on Intelligent Control and Automation, WCICA 2012, July 6, 2012 - July 8, 2012, 2012, pp. 4784-4790, Institute of Electrical and Electronics Engineers Inc., Beijing, China.
[14] S. Islam, R. Davies, M. Bennamoun and A. Mian, "Efficient detection and recognition of 3d ears", International Journal of Computer Vision, vol.95, no.1 2011, pp. 52-73.
[15] J. Zhou, S. Cadavid and M. Abdel-Mottaleb, "An efficient 3-d ear recognition system employing local and holistic features", IEEE TRANSACTIONS ON INFORMATION FORENSICS AND SECURITY, vol.7, no.3 2012.
[16] http://www.nd.edu/~cvrl/.
[17] http://www.mathworks.de/matlabcentral/fileexchange/8998.
[18] M. Pauly, M. Gross and L. P. Kobbelt, "Efficient simplification of point-sampled surfaces", in Visualization, 2002. VIS 2002. IEEE, 2002, pp. 163-170, IEEE.
[19] H. Hoppe, T. DeRose, T. Duchamp, J. McDonald and W. Stuetzle, "Surface reconstruction from unorganized points", SIGGRAPH Comput. Graph., vol.26, no.2 1992, pp. 71-78.
[20] M. Pauly, M. Gross and L. P. Kobbelt, "Efficient simplification of point-sampled surfaces", Proc. Proceedings of the conference on Visualization '02, Boston, Massachusetts2002, pp. 163-170.
[21] L. Wen-Jing and M. Zhi-Chun, "Ear detection based on improved adaboost algorithm", in Pattern Recognition, 2008. CCPR '08. Chinese Conference on, 2008, pp. 320-325.
[22] P. Yan and K. W. Bowyer, "Biometric recognition using 3d ear shape", IEEE Transactions on Pattern Analysis and Machine Intelligence, vol.29, no.8, Aug 2007, pp. 1297-1308.

Kai Wang received the B.E. degree from the School of Electrical Engineering at Henan Polytechnic University in 2005. He is currently pursuing Ph.D. in Control Science and Control Engineering from the School of Automation and Electrical Engineering, University of Science and Technology Beijing. His research interests include computer vision, pattern recognition, biometrics and machine learning.

Zhi-Chun Mu received the B.E. and M.E. degrees from the Department of Automation at University of Science and Technology Beijing in 1978 and 1983, respectively. He is currently a professor in the School of Automation and Electrical Engineering, University of Science and Technology Beijing. He was a visiting scholar at Davy International UK and Sheffield Polytechnic, England, from 1989 to 1991, and a visiting Professor at University of Brighton, England from 1996 to 1999. As a Guest Professor, he visited Laboratoire d'Electronique, d'Informatique et d'Image, CNRS University of Burgundy France in 2007. He was the Chair of Organizing Committee of IEEE International Conference on Wavelet Analysis and Pattern Recognition 2007. He has served as
a reviewer and member of Evaluation and Assessment Commission, Division of Information Science, National Natural Science Foundation of China since 2002.He is now Chair of IEEE SMC Beijing (capital region) Chapter. His main research interests include Pattern Recognition and Biometrics, Artificial Intelligence and its applications, Data Mining as well as Process Control and Modeling. He has published more than 180 refereed journal and conference papers in these areas. He is the corresponding author of this paper.